PNAS

Supplementary Information for:

A single-administration therapeutic interfering particle reduces SARS-CoV-2 viral shedding and pathogenesis in hamsters

Sonali Chaturvedi[1,2,†], Nathan Beutler[6,†], Michael Pablo[1,2,†], Gustavo Vasen[1,2], Xinyue Chen[1,2], Giuliana Calia[1,2], Lauren Buie[5], Robert Rodick[5], Davey Smith[7], Thomas Rogers[6,7,*], Leor S. Weinberger[1,2,3,4,*]

[†]these authors contributed equally

*to whom correspondence should be addressed: trogers@scripps.edu, leor.weinberger@gladstone.ucsf.edu

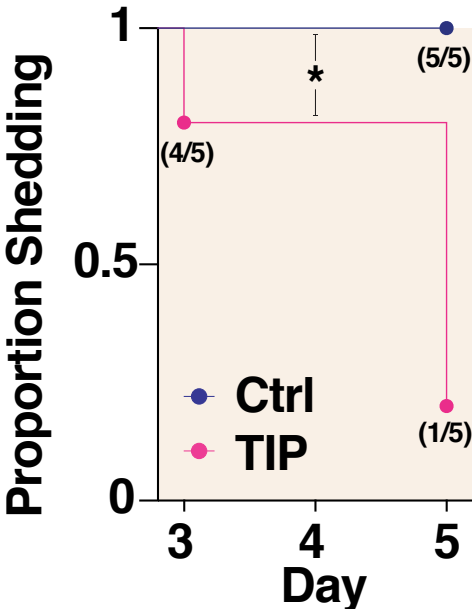**This PDF file includes:**
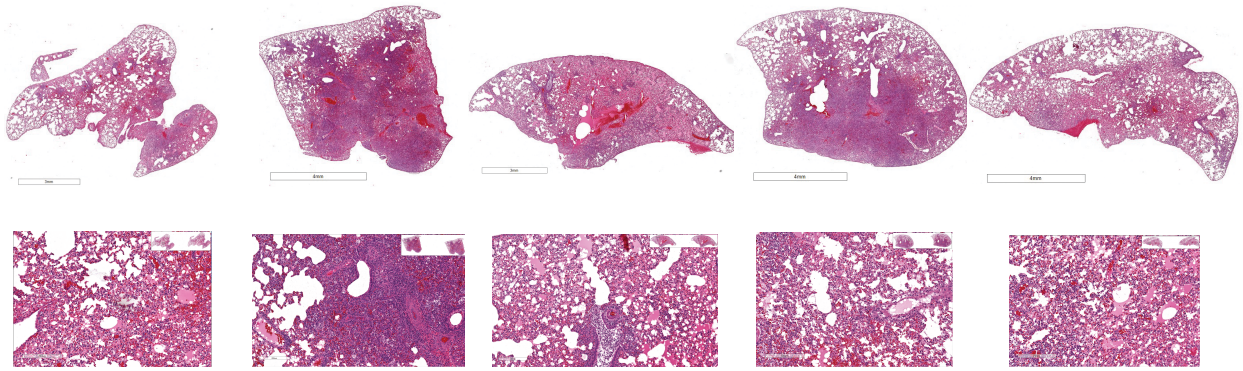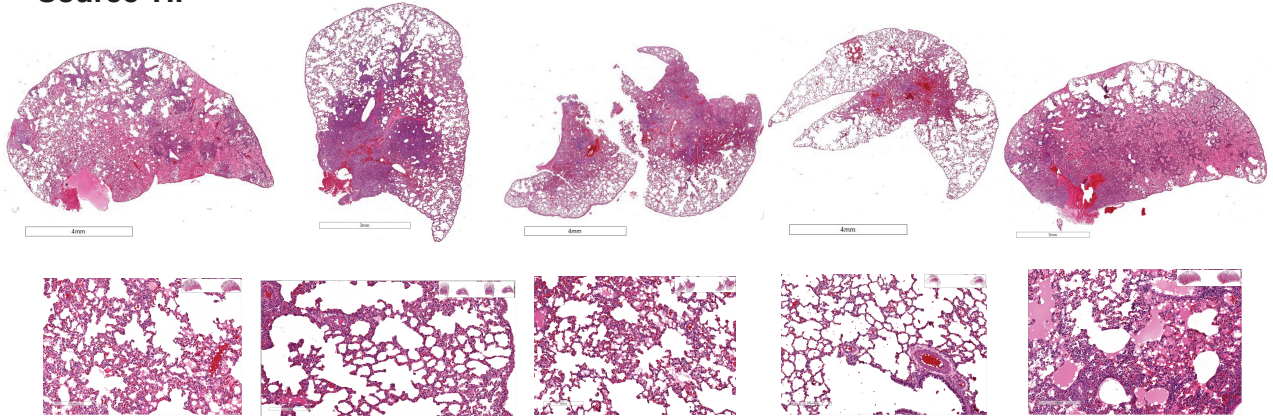
Supplemental Figure 1

Figure S1: Proportion of source hamsters shedding detectable virus quantified using the virus titer data in Fig. 1C and presented as a Kaplan-Meier plot. *, p<0.05 by Log-rank (Mantel-Cox) test.
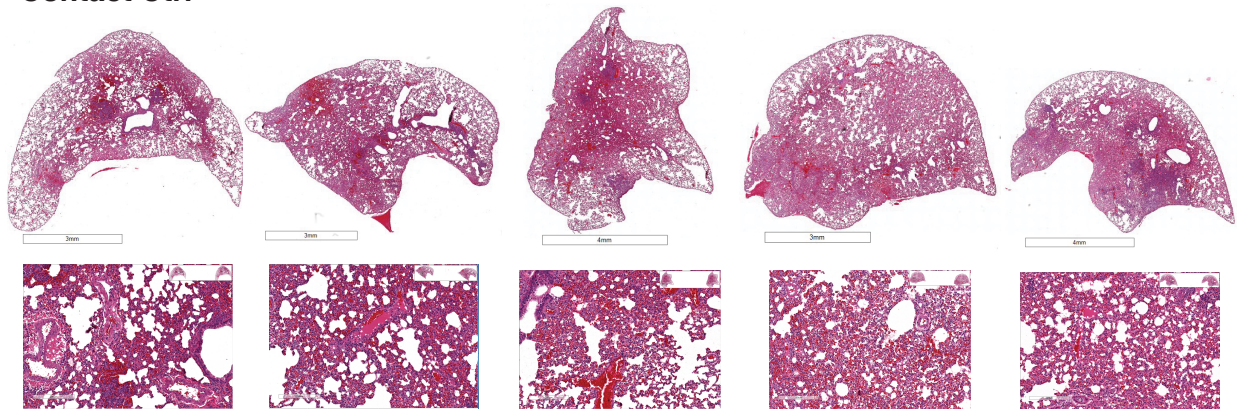
Supplemental Figure 2

Source Ctrl

Source TIP

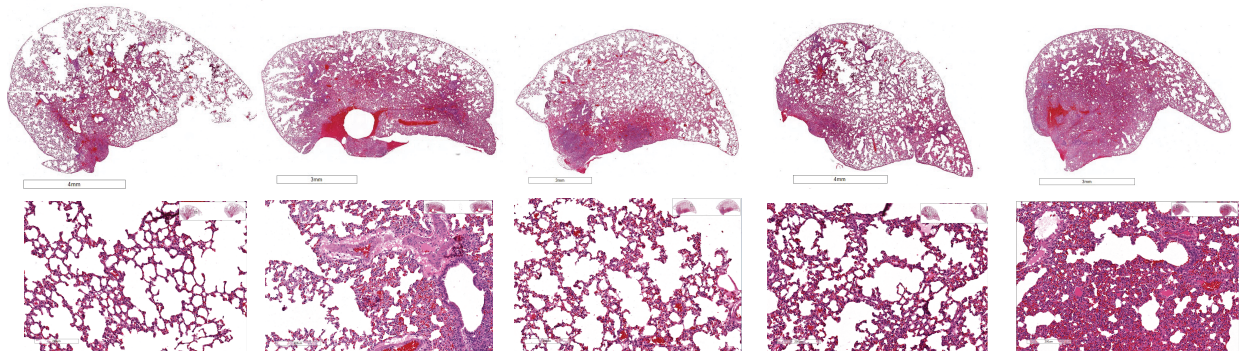

Contact Ctrl

Contact TIP

Figure S2.: Histopathology imaging of Syrian golden hamster lungs from source animals infected with SARS-CoV-2 (B.1.617.2) followed by intranasal Ctrl- or TIP-LNP treatment and their respective contact animals. Syrian golden hamsters (source) were intranasally infected with 10^6 PFU of SARS-CoV-2 (B.1.617.2), at 6 h post-infection, intranasal administration of TIP LNPs (n=5) or Ctrl RNA LNPs (n=5) was performed. At 36 h post-infection, uninfected and untreated hamsters (contact) were brought in direct contact with the source hamsters for 8 hours. At 44 h post-infection, source and contact hamsters were caged alone, lungs of source and contact animals were harvested at day 5 and day 6 respectively, fixed with Zn-formalin and histopathology was performed. Sticked images were analyzed using Leica Aperio ImageScope software. For each animal a representative zoomed-in section to visualize histopathology are shown. Micrographs of brightfield imaging of H&E-stained lung sections from all animals are shown (*first row*: Ctrl RNA treated source (n=5), *second row*: TIP RNA treated source (n=5), *third row*: contact hamsters cohoused with Ctrl-treated hamsters (n=5), *fourth row:* contact hamsters cohoused with TIP-treated hamsters (n=5)).
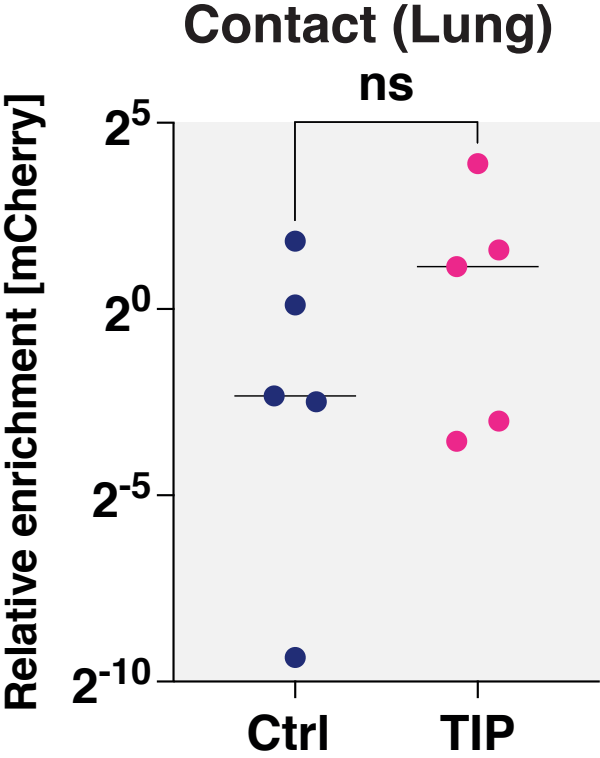
Supplemental Figure 3

Figure S3: No evidence for transmission of TIP to contacts from source animals infected with SARS-CoV-2 (B.1.617.2) followed by intranasal Ctrl- or TIP-LNP treatment. Lungs from contacts (at day 6) of TIP-treated (n=5) or Ctrl-treated (n=5) animals were harvested, homogenized, and qRT-PCR was performed for mCherry (TIP marker) and normalized to beta-actin. ns, $p > 0.05$.
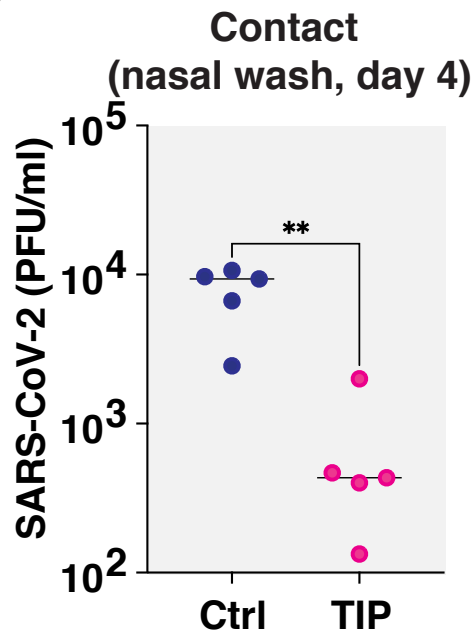
Supplemental Figure 4

Hamsters treated with TIPs at 12 hours post infection

A

B

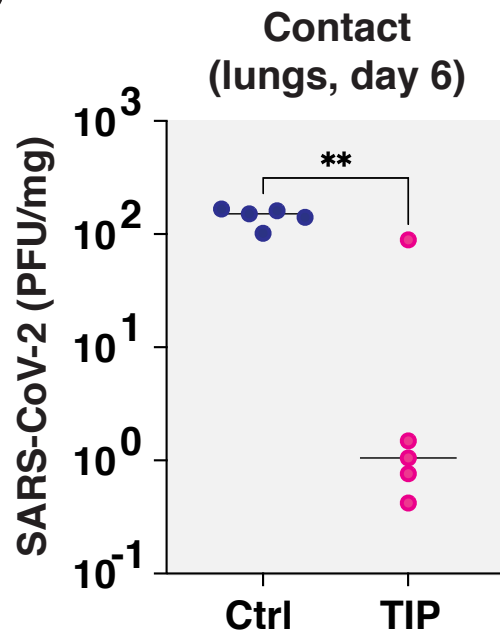**Contact (nasal wash, day 4)**

C

Contact (lungs, day 6)
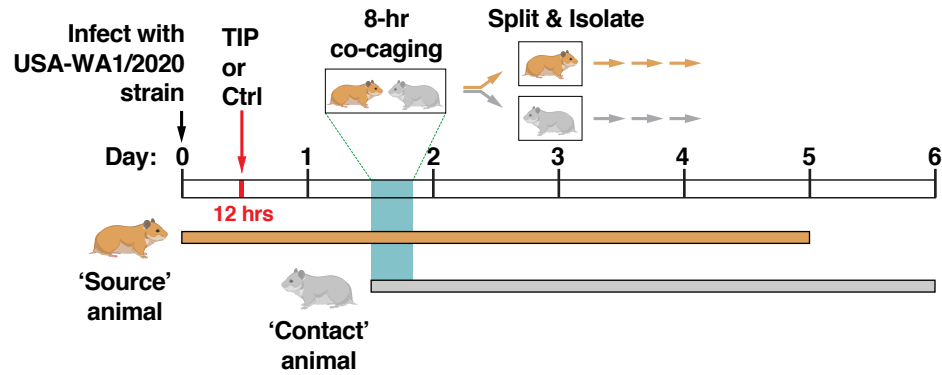
Figure S4: TIP treatment post-infection (USA-WA1/2020) results in lower viral shedding and reduced viral load in the lungs of contact animals. (A) Schematic of experimental design. Syrian golden hamsters (M/8-week-old) were intranasally infected with 10^6 PFU of SARS-CoV-2 (USA-WA1/2020) in 100µl of DMEM, as described (29). At 12-h post, hamsters were intranasally administered with 100µl of LNP solution containing either TIP RNA (n=5) or Ctrl RNA (n=5), at 36-h post infection, the source animals were co-caged with naïve animals (contact animals) for 8 hours, and all animals were caged individually starting 44-h post-infection. Nasal washes were collected for contact animals on day 3 and 4 followed by harvesting of lungs at day 6 (5 days after co-caging). **(B)** Exposure to TIP-treated animals reduces virus shedding in contacts, as measured by plaque assay of nasal washes from day 4. **(C)** Exposure to TIP-treated animals reduces infectious viral load in lungs of contacts, as compared to exposure to Ctrl-treated animals. Lungs from contacts were harvested, homogenized, and SARS-CoV-2 virus titer was quantified by plaque assay.

Supplemental Figure 5

A   Model error convergence
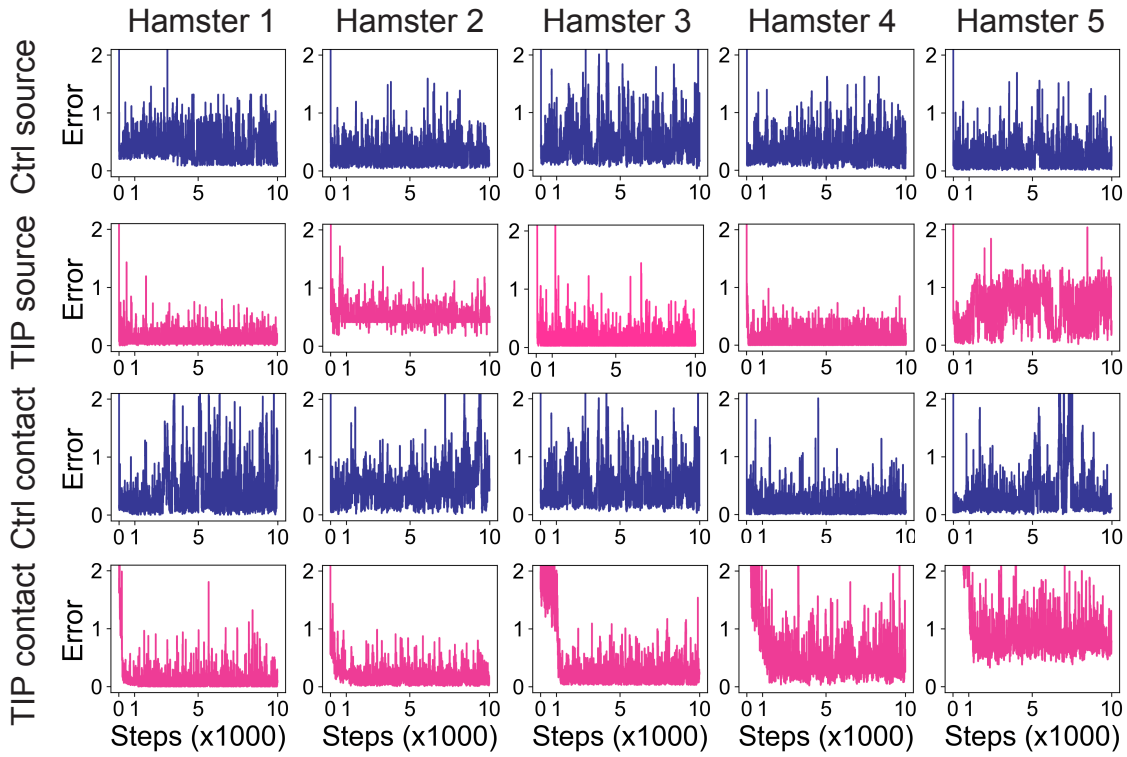
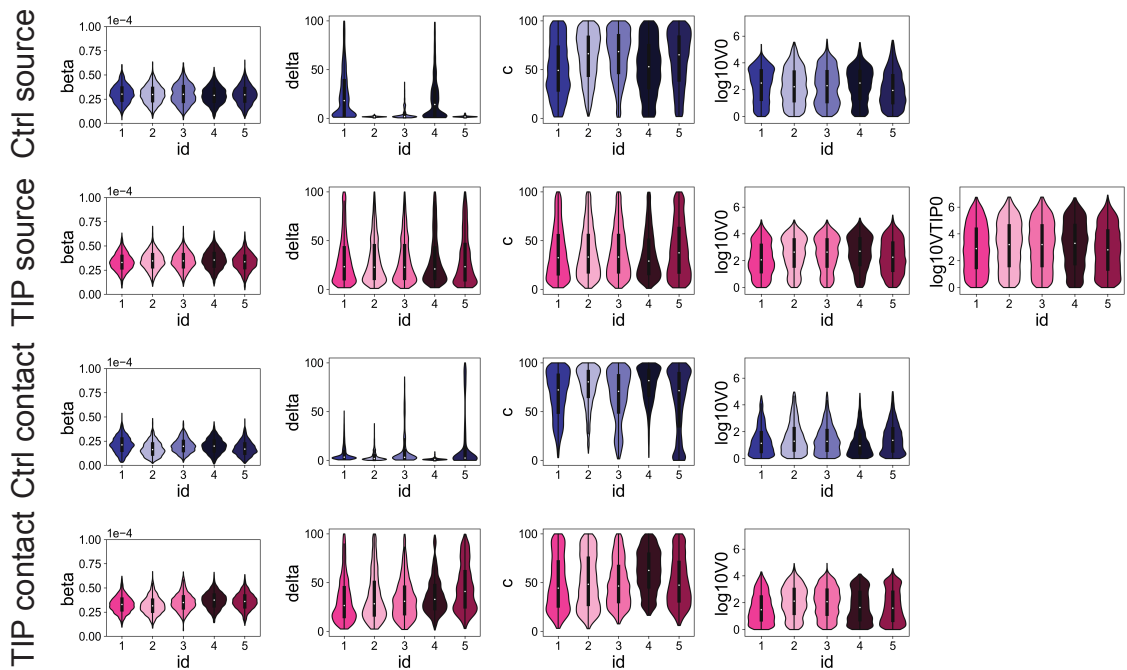## B   Model parameter distributions

Figure S5: Model fitting to source and contact hamster data. (A) Diagnostic plots across the 10,000 DRAM-MCMC steps, exhibiting convergence of fitting error. The first 1,000 steps are discarded as burn-in, and the posterior distribution (parameters, and median prediction, and predicted credible intervals) are generated by sampling from the remaining 9,000 steps. **(B)** The posterior parameter distributions indicate that the values of individual parameters have large uncertainty. Parameter uncertainty is likely due to both structural non-identifiability, driven by parameters compensating for one another with no impact on the observed variable, and practical non-identifiability, driven by variation inherent in the data, and limited availability of time points.

Table S1. List and sequences of oligonucleotides used in the study.

1	N gene qpcr	fw: aaattttgggggaccaggaac rev:tggcacctgtgtaggtcaac
2	b-actin (M. auratus) qpcr	fw: actgccgcatcctcttcct rev: tcgttgccaatggtgatgac
3	IL6 (M. auratus) qPCR	fw: ggtatgctaaggcacagcacact rev cctgaaagcacttgaagaattcc
4	IL10 (M. auratus) qPCR	fw: gaaggaccagctggacaaca rev:tggcaacccaagtaacccctta
5	TNF (M. auratus) qPCR	fw: ggagtggctgagccatcgt rev:agctggttgtctttgagagacatg
6	IL1-beta (M. auratus) qPCR	fw: ggctgatgctcccattcg rev: cacgaggcatttctgttgttca
7	CCL20 (M. auratus) qPCR	fw: agtcagtcagaagcaagcaact rev: tgaagcggtgcatgatcc
8	IL4 (M. auratus) qPCR	fw: ccacggagaaagacctcatctg rev: gggtcacctcatgttggaaataaa
9	IL10 (M. auratus) qPCR	fw: gttgccaaaccttatcagaaatga rev: ttctggcccgtggttctct
10	IL2 (M. auratus) qPCR	fw: gtgcacccacttcaagctctaa rev:aagctcctgtaagtccagcagtaac
11	CXCL10 (M. auratus) qPCR	fw: gccattcatccacagttgaca rev: catggtgctgacagtggagtct
12	ISG15 (M. auratus) qPCR	fw: tctatgaggtccggctgaca rev: gcactggggctttaggtcat
13.	IFN- gamma (M. auratus) qPCR	fw: ggccatccagaggagcatag rev: tttctccatgctgctgttgaa
14.	TIPs PCR primers	t7 fw: taatacgactcactatagggattaaaggtt rev: ttttttttttttttttttgtcattctcctaagaagc
15.	mCherry qPCR	fw: gaacggccacgagttcgaga rev: cttggagccgtacatgaactgagg